Applied Catalysis B: Environmental 91 (2009) 101–107

Contents lists available at ScienceDirect

Applied Catalysis B: Environmental

journal homepage: www.elsevier.com/locate/apcatb

Oxidative methanol steam reforming on a highly dispersed $CuO/CeO_2/Al_2O_3$ catalyst prepared by a single-step method

Maria Turco [a,*], Claudia Cammarano [a], Giovanni Bagnasco [a], Elisa Moretti [b], Loretta Storaro [b], Aldo Talon [b], Maurizio Lenarda [b]

[a] Dipartimento di Ingegneria Chimica, Università di Napoli Federico II, P.le V. Tecchio, 80125 Napoli, Italy
[b] INSTM UdR Venezia-Dipartimento di Chimica, Università Ca' Foscari di Venezia, Via Torino 155/b, 30172 Mestre, Venezia, Italy

ARTICLE INFO

Article history:
Received 23 February 2009
Received in revised form 5 May 2009
Accepted 10 May 2009
Available online 19 May 2009

Keywords:
Oxidative methanol steam reforming
$Cu/CeO_2/Al_2O_3$ catalysts
Organized mesostructured alumina
Cu dispersion

ABSTRACT

A $Cu/CeO_2/Al_2O_3$ catalyst (6.6% Cu, 13.8% Ce) based on a structurally organized mesoporous alumina was prepared by a new single-step sol–gel method starting from Al butoxide and Ce and Cu stearates. The sample was characterized by N_2 adsorption, XRD, TPR and Cu dispersion measurements and tested as catalyst for the SRM (methanol steam reforming) and OSRM (methanol autothermal reforming) reactions. The material showed a huge surface area (360 $m^2\ g^{-1}$) and resulted to contain very dispersed CeO_2 and CuO phases on a poorly crystalline alumina matrix. A highly dispersed Cu metallic phase was obtained after a reductive treatment with H_2. Catalytic tests showed that the unreduced material was fairly active for the OSRM process, but the activity increases appreciably after the pre-reduction treatment. The activity for the OSRM process resulted high, in terms of hydrogen production rate, if compared with data on similar Cu/Ce/Al systems, but the activity for SRM, in the absence of oxygen was, on the other hand, very low. This behaviour was explained either considering the occurrence of H spillover or the CeO_2 assisted oxidation of Cu to Cu^+.

1. Introduction

Proton-exchange membrane fuel cells (PEMFCs) are being actively considered as most suitable and commercially viable hydrogen-based fuel cell systems for static and mobile applications [1,2]. Even if pure hydrogen would be very convenient as fuel cell feed, its use for mobile applications has serious disadvantages caused by distribution and storage difficulties. Alternatively, hydrogen can be produced on-board from various suitable hydrocarbon sources [3,4]. Methanol is preferable to other liquid hydrocarbons because it is readily available, has high hydrogen to carbon ratio and can be converted to H_2-rich gas by reforming at relatively low temperature [5,6]. Hydrogen can be produced from methanol by steam reforming (SRM, reaction (1)) and partial oxidation (POM, reaction (2))

$$CH_3OH_{(g)} + H_2O_{(g)} = CO_2 + 3H_2 \qquad \Delta H^\circ = 49.5\ kJ\ mol^{-1} \tag{1}$$

$$CH_3OH_{(g)} + \tfrac{1}{2}O_2 = CO_2 + 2H_2 \qquad \Delta H^\circ = -192.3\ kJ\ mol^{-1} \tag{2}$$

The combination of the endothermic (1) and the exothermic (2) reactions gives rise to oxidative steam reforming (OSRM), that is potentially an autothermal process and can give some advantages such as a smaller reactor volume and a simpler reactor design [7].

The reaction network of this process is very complex and not yet well defined. In the reacting system, besides SRM and POM, other reactions can also occur such as dehydration, dehydrogenation, decomposition, combustion and water gas shift (WGS) [8,9]. Among the by-products, the presence of CO is most undesired because even low CO concentrations (>20 ppm) cause the poisoning of the platinum anodes of PEMFCs. High purity H_2 for feeding PEMFCs requires the elimination of CO by proper purification processes: generally water gas shift (WGS, reaction (3)) followed by preferential CO oxidation (PROX, reaction (4)) is employed for this purpose [10,11].

$$CO + H_2O \rightarrow CO_2 + H_2 \tag{3}$$

$$CO + \tfrac{1}{2}O_2 \rightarrow CO_2 \tag{4}$$

WGS allows to reduce the CO concentration in the reformed gas to about 0.5% while PROX allows further reduction to less than 10 ppm. These processes add complexity and cost to the methanol reformer, therefore there is great interest in developing highly selective catalysts that minimize the production of CO.

* Corresponding author. Tel.: +39 0817682259; fax: +39 0815936936.
E-mail addresses: turco@unina.it (M. Turco), lenarda@unive.it (M. Lenarda).

0926-3373/$ – see front matter © 2009 Elsevier B.V. All rights reserved.
doi:10.1016/j.apcatb.2009.05.011

The catalysts employed for SRM and OSRM are generally based on metallic Cu or Pd. Palladium catalysts have higher thermal stability [12–14] but lower selectivity, because they also activate methanol decomposition, producing noticeable amounts of CO [13,15–18]. Copper-containing catalysts show a particularly high activity and selectivity for SRM and OSRM. The most studied catalysts to date are based on Cu/ZnO [19–25], and $Cu/ZnO/Al_2O_3$ [8,9,23,24,26–30] obtained by reduction of oxides precursor systems.

Recently, new Cu/CeO_2 based catalysts have been considered for SRM and OSRM [31–35]. These systems have interesting catalytic properties due to the high oxygen mobility of CeO_2, high dispersion of metallic Cu and strong metal-support interaction (SMSI) [33,34,36–38]. The formation of a solid solution $Ce_{1-x}Cu_xO_{2-x}$ can lead to highly dispersed Cu metal particles after reduction [35]. These catalysts were studied for several oxidation processes such as water gas shift (WGS) [39,40], low-temperature carbon monoxide oxidation [41–43], phenol wet oxidation [44]. Moreover they appeared particularly active and selective for the CO PROX process [45–49]. This suggests that the presence of CeO_2 in Cu based catalysts should lead to a significant suppression of CO formation in OSRM. Moreover other advantages can be expected: the presence of ceria hindering Cu sintering can enhance the thermal stability [50] and can also increase the long term stability because the oxygen storage capacity of CeO_2 favours coke gasification [32].

Cu/CeO_2 catalysts can be prepared by different methods, that is impregnation, co-precipitation, sol–gel synthesis, hydrothermal synthesis, decomposition or combustion of suitable precursor compounds: catalytic properties depend strongly on the preparation procedure of the precursor oxides [35,36,48,51,52].

In a previous work a new surfactant-assisted single-step sol–gel method was presented for the preparation of Cu/Ce catalysts supported on alumina [49]. This method allowed to obtain oxide systems characterized by a structurally organized mesoporosity, with high surface area and good thermal stability, exhibiting interesting catalytic activity for the PROX reaction [49]. In this paper a $CuO/CeO_2/Al_2O_3$ catalyst prepared by this new approach is characterized and studied for the SRM and OSRM processes with the aim of investigating on the possibility of employing these systems as selective catalysts for the OSRM process.

2. Experimental

2.1. Preparation of the catalyst

All chemicals were purchased from Aldrich and used without further purification.

The reagents were employed in the preparation of the catalyst in the following molar ratio: 1 $Al(sec\text{-}BuO)_3$:0.053 $(C_{17}H_{35}COO)_3Ce$:0.072 $(C_{17}H_{35}COO)_2Cu$:24 n-C_3H_7OH:3H_2O. Cu and Ce stearates were prepared as described in a previous work [53].

The required amounts of Ce and Cu stearates were dissolved in n-propanol by sonication. After addition of deionized water, the solution was stirred for 30 min. Then aluminium tri-sec-butoxide was added and the reaction mixture was stirred for further 30 min. The resulting suspension was aged for 50 h in a Teflon-lined autoclave at 100 °C and autogenous pressure. After cooling to room temperature, the product was recovered by centrifugation, washed with ethanol and dried at 50 °C overnight. Then it was thermally treated up to 410 °C in nitrogen flow (heating rate 3 °C min^{-1}), kept at this temperature for 6 h and heated at 550 °C in a stream of air (heating rate 3 °C min^{-1}) for 5 h. The calcination temperature of 550 °C was selected to completely remove the organic material as indicated by TG analysis. The sample was ground and sieved to 100–140 mesh. Cu was reduced to the metallic state in situ by treating the sample at a rate of 10 °C min^{-1} up to 450 °C and then keeping it at 450 °C for 2 h in a flow of 2% H_2/Ar mixture. The chemically analyzed catalyst resulted to contain 13.8% Ce and 6.6% Cu and was identified as $EMCe_{14}Cu_7$ (16.9% CeO_2, 8.3% CuO, 74.79% Al_2O_3). The reference material CuO (S_{BET} = 30 m^2 g^{-1}) was supplied by Aldrich.

2.2. Characterization of the catalyst

N_2 adsorption–desorption measurements were performed at liquid nitrogen temperature (−196 °C) with an ASAP 2010 apparatus from Micromeritics on samples outgassed at 130 °C. Specific surface areas were determined by the BET equation, and specific pore volumes were calculated at p/p_0 = 0.98. The pore size distribution was calculated following the BJH method, assuming a cylindrical pore model.

X-ray diffraction patterns were obtained with a Bragg–Brentano powder diffractometer using CuKα radiation (λ = 1.54184 Å) and a graphite monochromator in the diffracted beam. The samples were disc shaped pressed powders. The average dimension of the crystallites was determined by the Scherrer equation.

TPR was carried out in a 2% H_2/Ar mixture at rate of 10 °C min^{-1} up to 450 or 600 °C (as indicated below), keeping the sample at the final temperature for 2 h.

Cu dispersion was measured by the N_2O chemisorption method [49]. The sample reduced after a standard TPR run was superficially oxidized to Cu_2O by treatment in N_2O flow at 60 °C. Then a further TPR run (from 60 to 600 °C, rate = 10 °C min^{-1}) allowed to determine the amount of $Cu_2O_{(surf)}$ and then the amount of $Cu_{(surf)}$ and the Cu dispersion, defined by: Cu dispersion = 100$Cu_{(surf)}$/Cu total. The Cu surface area and Cu particle sizes were calculated assuming a surface Cu concentration of 1.47×10^{19} atoms m^{-2} [54].

2.3. Catalytic activity measurements

Catalytic tests were carried out in a laboratory flow apparatus schematically represented in Fig. 1. The apparatus employed a

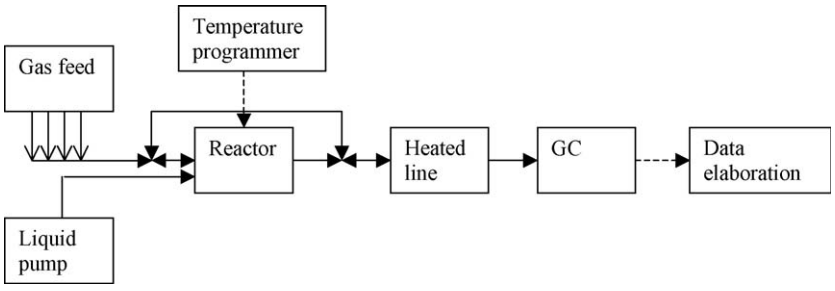

Fig. 1. Apparatus for OSRM and SRM tests.

fixed bed reactor operating at atmospheric pressure. The catalyst (mass = 0.09 g, size = 90–110 μm) was diluted with fused quartz powder in 1:10 ratio to guarantee isothermal conditions. Before starting the test, the catalyst was pre-reduced in situ as described in Section 2.1. The liquid feed (H_2O/CH_3OH) was regulated by a Varian HPLC metering pump and the gaseous feed (O_2, He) by Brooks electronic mass flow controllers. The reaction products were sent through a heated line to a gas-chromatograph HP 5890 equipped with a double-packed Porapak-molecular sieve column and a TCD detector. Products analyzed were H_2, CO (detection limit = 0.01%), CO_2, O_2, CH_4, CH_3OH, H_2O. Methanol total conversion and partial conversions to different products were calculated from concentrations in the effluent stream, taking into account the volume variation due to the reactions. H_2 yield was calculated as the ratio between mol H_2 produced and mol CH_3OH fed. Mass balances of C, H and O were fulfilled within ±5%. A Hiden mass spectrometer was employed for the identification of products not detected by GC. OSRM tests were carried out at T = 200–400 °C, $H_2O/CH_3OH/O_2$ molar ratios = 1.1/1/0.12, (CH_3OH concentration = 17.8%), WHSV = 60 L h^{-1} g^{-1} (helium as balance). SRM tests were carried out under similar conditions, but excluding O_2. Each test lasted 1.5–2 h and during this time the products were sampled and analyzed two or three times to verify that constant conversion values were attained. Preliminary tests were carried out to ascertain that diffusive resistances were negligible.

3. Results and discussion

3.1. N_2 adsorption

The results of N_2 adsorption measurements are reported in Table 1. The sample shows a Type IV isotherm with a hysteresis loop typical of mesoporous materials, as expected for this type of materials [49]. BET surface area of calcined sample are very high and seems neither affected by the reduction with H_2 nor by operating under reaction conditions. Such treatments have also no influence on pore volume and pore size distribution.

3.2. XRD analysis

The diffractogram of $EMCe_{14}Cu_7$ (Fig. 2) exhibits broad reflections due to γ-alumina, with a poorly microcrystalline structure, and peaks attributable to the presence of CeO_2 with a fluorite lattice structure. The average dimension of the ceria crystallites, calculated from the main peak at $2\theta = 28.6°$, according to the Scherrer's equation, resulted about 3.0 nm. The presence of a broad and very weak peak at $2\theta = 35.54°$ characteristic of the tenorite could indicate a CuO phase highly dispersed on the ceria and alumina surface with particles dimension near the XRD detection limit. As reported below, copper dispersion measured by N_2O chemisorption is very high, confirming the effectiveness of the preparation method in obtaining highly dispersed copper phases.

Table 1
Surface area, pore volume and pore diameter of $EMCe_{14}Cu_7$ samples calcined, reduced in H_2 and tested in OSRM.

Sample treatment	S_{BET}[a] (m^2 g^{-1})	V_p[b] (cm^3 g^{-1})	D_p[c] (nm)
Calcined 550 °C	360	0.48	3.9
Reduced 450 °C	345	0.47	3.9
Used in OSRM	330	0.45	4.0

[a] BET specific surface area.
[b] Specific pore volume determined at $p/p^\circ = 0.98$.
[c] Pore diameter evaluated by BJH method.

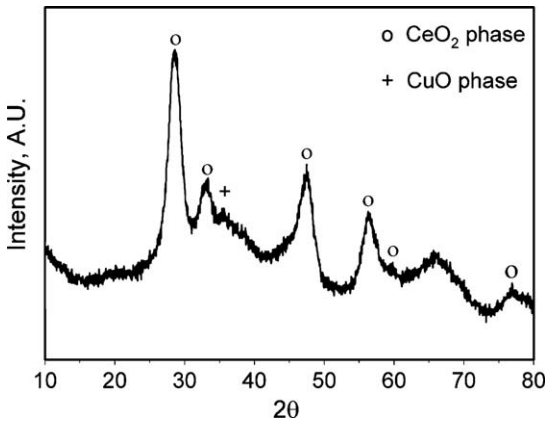

Fig. 2. X-ray diffraction pattern of the catalyst $EMCe_{14}Cu_7$, after thermal treatment in air at 550 °C.

3.3. TPR measurements

The TPR spectrum of the $EMCe_{14}Cu_7$ sample and of the reference material CuO after pretreatment in air at 500 °C are shown in Fig. 3, together with the spectrum of the catalyst $EMCe_{12}Cu_4$, containing 11.8%Ce and 3.6%Cu, previously studied for the CO-PROX reaction [49], that is reported for comparison. The corresponding amounts of consumed H_2, calculated from the peak areas, are reported in Table 2.

The reference material CuO gives a TPR peak at 400 °C, with intensity corresponding to the complete reduction to Cu^0. The catalyst $EMCe_{14}Cu_7$ shows a composite spectrum with at least three components at temperatures close to those of the sample $EMCe_{12}Cu_4$ (maxima at 176, 292 and 428 °C), but with higher intensity. The TPR profile of the catalyst shows no signal at the temperatures usually found for CeO_2 [49,55–57], indicating that the oxide probably is highly dispersed on alumina, and in this form can undergo a partial reduction at about 450 °C [49,57]. Moreover the TPR profile of the catalyst indicates that most Cu is not present as bulk CuO, but as more reducible species. Taking into account the similarity with the TPR profile of the $EMCe_{12}Cu_4$ sample and previous TPR data on similar materials [58], the signal at 176 °C, due to very reducible species, can be attributed to Cu^{2+} ions or small clusters tightly bonded to CeO_2, while the TPR signal at 292 °C is probably due to a well dispersed CuO phase, that is CuO nanometric particles dispersed on alumina. The TPR signal at high temperature can be attributed to the reduction of larger CuO particles: however also some reduction of CeO_2 dispersed on

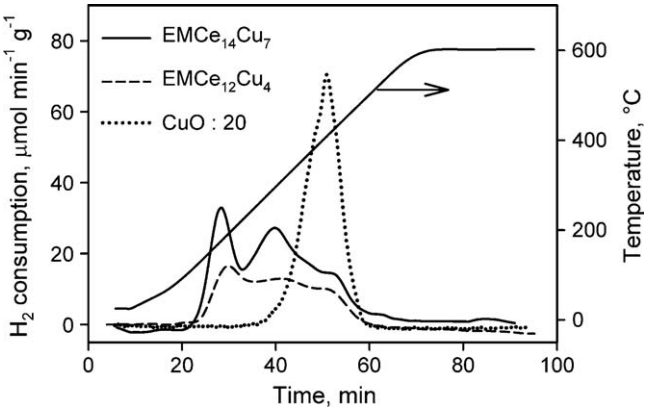

Fig. 3. TPR profile of the catalyst $EMCe_{14}Cu_7$ compared with those of the catalyst $EMCe_{12}Cu_4$ (Ref. [48]) and of the reference material CuO. Note the different scale for CuO.

Table 2
TPR measurements.

Sample	H_2 consumed (mmol g^{-1})	Cu content (mmol g^{-1})	H_2 consumed/ Cu content
$EMCe_{14}Cu_7$	0.69	1.04	0.66
$EMCe_{12}Cu_4$[a]	0.377	0.58	0.65
CuO	12.5	12.5	1.00

[a] Data from Ref. [49].

alumina can contribute to this signal. In fact a partial reduction of CeO_2 at about 450 °C occurred in the corresponding CeO_2/Al_2O_3 system [49]. Some tailing at high temperature could be due to the slow reduction of Cu^+ species, that are strongly stabilized by interaction with the CeO_2 phase. The presence of Cu^+ species forming part of Cu-O-Ce sites was previously observed on a similar catalyst by XPS measurements [49]. Moreover the stabilizing effect of CeO_2 on the oxidation state Cu^+ was suggested in other studies [35,59]. Compared with the previous $EMCe_{12}Cu_4$, the TPR profile of the sample $EMCe_{14}Cu_7$ shows higher intensity of all signals, clearly due to higher Cu content: it is worth noting that mainly the low and medium temperature signals increase: this suggests that increasing Cu content, instead of increasing the amount of bulk CuO, leads to an increase of the Cu fraction present as isolated Cu^{2+} ions or CuO tightly bonded to CeO_2 or dispersed on alumina.

Table 2 shows that the amount of consumed H_2 is lower than that corresponding to complete reduction of Cu^{2+} to Cu^0. Since it is unlikely that Cu is not completely reduced to the metallic state under these conditions, this means that the average initial oxidation state of Cu is lower than 2, precisely 1.33. Thus the air treated sample appears to contain both Cu^{2+} and Cu^+: this can be related to the stabilizing effect of CeO_2 on the Cu^+ species [35].

3.4. Cu dispersion

In Fig. 4 we report the TPR profile obtained with the catalyst $EMCe_{14}Cu_7$ reduced and treated with N_2O as described above (see Section 2) together with, for sake of comparison, the corresponding profile obtained with the previously studied $EMCe_{12}Cu_4$ sample.

The TPR signals occur at low temperatures (maxima at 148 and 194 °C) as expected for the reduction of surface Cu_2O. The Cu surface area of $EMCe_{14}Cu_7$ calculated from the amount of H_2 consumed is 29.4 $m^2\ g^{-1}$, corresponding to a Cu dispersion of 69%. This very high dispersion is in agreement with the results of the XRD analysis indicating very high dispersion of Cu oxide. It is also interesting the presence of two TPR signals at 148 and 194 °C attributable to surface Cu_2O: such behavior, that was observed, but

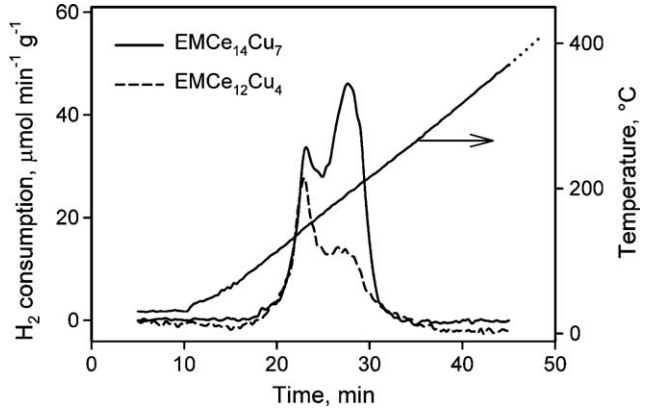

Fig. 4. TPR profile obtained on the sample $EMCe_{14}Cu_7$ reduced and superficially oxidized with N_2O, compared with that obtained with the previous material $EMCe_{12}Cu_4$.

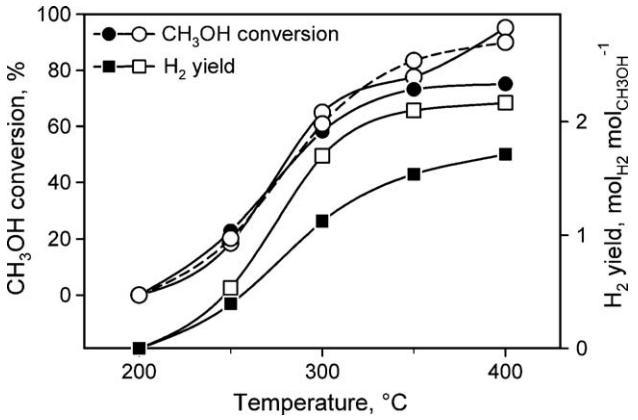

Fig. 5. CH_3OH conversion and H_2 yield in the OSRM tests. Empty symbols (○, □): catalyst pre-reduced with H_2; full symbols (●, ■): catalyst not pre-reduced. Dashed line: repeated tests.

with lower evidence for different Cu catalysts [8], is probably due to the presence of a mesostructured, very high surface area alumina. It can be hypothesized that water produced by reduction of Cu_2O is released from the material with a slow diffusion–adsorption sequence occurring in the tortuous mesopores system of alumina. It is likely that water vapor can re-oxidize Cu^0 under these conditions [9], so the slow H_2O desorption can cause a delay in Cu reduction, leading to a tailing of the TPR signal or even the appearance of a further TPR signal. This effect is more pronounced with these Cu/Ce/Al materials probably because of several co-operating factors such as very high surface area, mesoporous structure, high Cu dispersion. However, it does not affect the calculation of the Cu surface area, since it is clear from an hydrogen–oxygen balance that the total amount of H_2 consumed must correspond to the oxygen originally adsorbed on Cu. If this is the correct interpretation, the data in Fig. 4 show that this effect is stronger for the sample $EMCe_{14}Cu_7$ than for the older material, probably due to the larger amount of H_2O produced (due to the higher Cu oxide content), or to the higher fraction of Cu crystallites located inside the alumina pores.

3.5. Catalytic tests

Data of the $EMCe_{14}Cu_7$ sample catalytic activity tests of OSRM in the 200–400 °C temperature range are reported in Figs. 5–7. The tests were carried out both on the catalyst pre-reduced with H_2 (see Section 2), and on the not pre-reduced, only pre-treated in air at 550 °C sample.

It can be observed that the methanol conversion increases regularly with temperature according to S-shaped curves, being slightly higher for the pre-reduced catalyst. The pre-reduction of the catalyst has a more evident effect on the H_2 yield: for the pre-reduced catalyst H_2 yield increases with temperature up to a value of 2.2 mol_{H_2} mol CH_3OH^{-1} at 400 °C, while for the not pre-reduced one it reaches at the same temperature the value of only 1.75 mol_{H2} mol_{CH3OH}^{-1}. As shown in Figs. 5 and 6, conversion to CO_2 value is close to that of the CH_3OH conversion for the pre-reduced sample, indicating that the contribution of side reactions is low. However some CO is also produced: the conversion to CO strongly increases with the temperature, reaching 7% at 400 °C. In the case of the not pre-reduced sample, the conversion to CO_2 parallels but is appreciably lower than CH_3OH conversion, indicating that the contribution of the secondary reactions is not negligible: the conversion to CO increases rapidly with the temperature, above 300 °C also for this catalyst, reaching about 4% at 400 °C. In Fig. 7 the conversions to $(CH_3)_2O$ and CH_2O are reported.

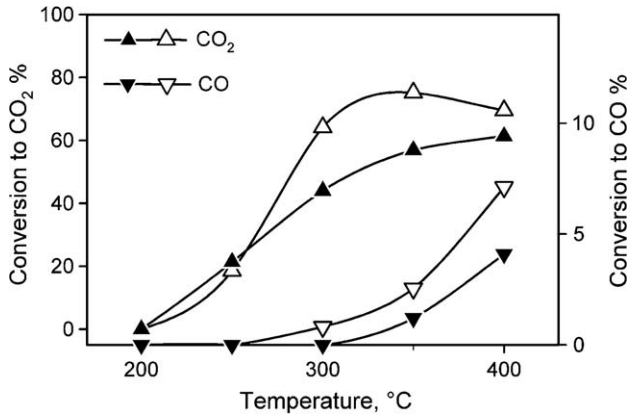

Fig. 6. CH_3OH conversion to CO_2 and CO in the OSRM tests. Empty symbols (▽, △): catalyst pre-reduced with H_2; full symbols (▼, ▲): catalyst not pre-reduced.

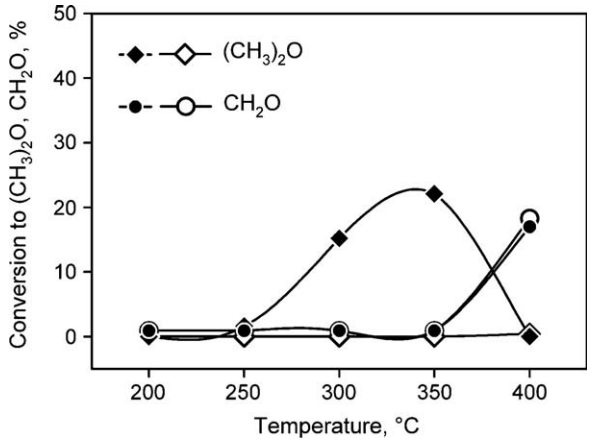

Fig. 7. CH_3OH conversion to $(CH_3)_2O$ and CH_2O in the OSRM tests. Empty symbols (◇, ○): catalyst pre-reduced with H_2; full symbols (◆, ●): catalyst not pre-reduced.

Both the pre-reduced and not pre-reduced materials produce CH_2O only at 400 °C, the amount of this product being higher for the not pre-reduced one. No $(CH_3)_2O$ is observed with the pre-reduced catalyst, while this compound is observed in noticeable amounts with the not pre-reduced sample in the 300–350 °C range, being, on the other hand, negligible at lower and higher temperatures.

The series of OSRM tests was repeated in the same sequence 200-400 °C, obtaining the same values of activity as in the first cycle (Fig. 5): this allows to exclude deactivation phenomena, at least during the time of catalytic tests.

It is interesting to compare the OSRM activity of this catalyst with that of similar Cu and Ce based systems presented in the literature, although the number of such studies is very limited. The most suitable for this comparison are those by Patel and Pant [38,60] reported in Table 3, that refer to H_2 pre-reduced catalysts. The activity of the catalyst $EMCe_{12}Cu_4$ appear high if compared with these data, considering that the catalyst in Ref. [60] contains also Zn as promoter. Shan et al. [61] studied the OSRM over a not reduced Cu/Ce catalyst that we compare with the not reduced $EMCe_{14}Cu_7$ sample. As shown in Table 3, the comparison favours our system also in this case, and even more if the lower Cu content is taken into account.

Since it is known that metallic copper is required for methanol reforming [8], the significant reforming activity found on the not pre-reduced catalyst indicates that, even if metallic Cu is not present initially in the catalyst, it is formed under reaction conditions. It can be hypothesized that the reduction of Cu oxide to the metallic state occurs simply through the reducing effect of methanol, analogously to what occurs in the so called "polyol" reduction of copper cations [62,63].

Another explanation can be that the initially present Cu oxide activates the partial oxidation of methanol producing H_2, and then H_2 reduces Cu oxide to metallic Cu. However the Cu^0 phase obtained in this way is less active than that formed by the H_2 reducing pre-treatment, as pointed by the lower H_2 yield. This can be due either to not complete reduction of Cu oxide or to formation of a less dispersed metallic phase.

The catalyst, in order to obtain a better knowledge of its properties, was tested also for the simple steam reforming of methanol (SRM), that is with the same flow rates of CH_3OH and H_2O, but in the absence of oxygen in the reaction system. The results of these tests, that were carried out both on the catalyst reduced with H_2 and on the not reduced one, are shown in Figs. 8–10.

It appears evident that under SRM conditions the behavior of the H_2 pre-reduced catalyst is the same as that of the not pre-reduced sample. Moreover Fig. 8 shows that the methanol conversion is always lower than under OSRM conditions (Fig. 5). In particular the H_2 yield appears much lower, indicating very low SRM activity. It can be noted that the maximum H_2 yield ($0.5\ mol_{H2}\ mol_{CH3OH}^{-1}$) corresponds to only 16% conversion of methanol through steam reforming. This low activity is confirmed by the low values of conversion to CO_2, as appears from Fig. 9. Conversion to CO starts above 300 °C and reaches a noticeable value at 400 °C (Fig. 9). In Fig. 10 the conversion of methanol to formaldehyde and dimethyleter under SRM conditions is shown.

The conversion to CH_2O is negligible in the entire temperature range for both samples, while the conversion to $(CH_3)_2O$ is less than 20% at 200–250 °C and increases with temperature up to 40% at 400 °C. Thus it clearly appears that under SRM conditions the main product is dimethylether. This means that under these conditions the methanol dehydration largely prevails on steam reforming both with the pre-reduced catalyst and with the not pre-reduced one. The high activity for methanol dehydration can be

Table 3
Comparison of data from OSRM tests.

Author [reference]	Catalyst composition Cu/Ce/Al (atom %)	Feed ratio $O_2/H_2O/CH_3OH$	WHSV ($L\ g^{-1}\ h^{-1}$)	Temperature (°C)	H_2 production rate ($\mu mol\ s^{-1}\ g_{cat}^{-1-}$)
Present work[a]	6/6/88	0.12/1.1/1	60	300	210
Present work[b]	6/6/88	0.12/1.1/1	60	300	135
Patel and Pant [38][a]	19/6/75	0.15/1.5/1	5.7[c]	280	180
Patel and Pant [60][a]	20/3/64[d]	0.15/1.5/1	7.8[c]	300	240
Shan et al. [61][b]	10/90/0	0.3/1.3/1	20	300	110

[a] Catalyst pre-reduced with H_2.
[b] Catalyst not pre-reduced.
[c] Referred to CH_3OH flow.
[d] Containing 13 mol% Zn.

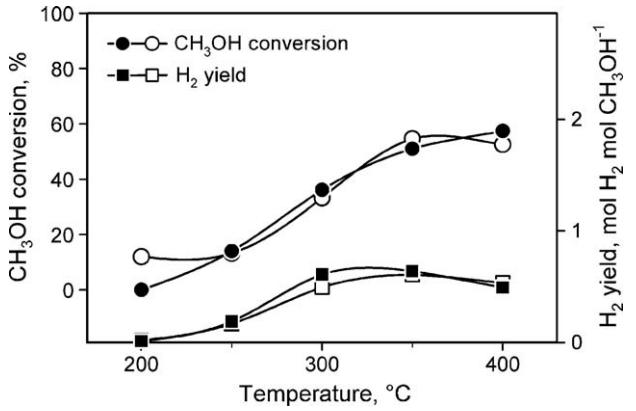

Fig. 8. CH_3OH conversion and H_2 yield in the SRM tests. Empty symbols (○, □): catalyst pre-reduced with H_2; full symbols (●, ■): catalyst not pre-reduced.

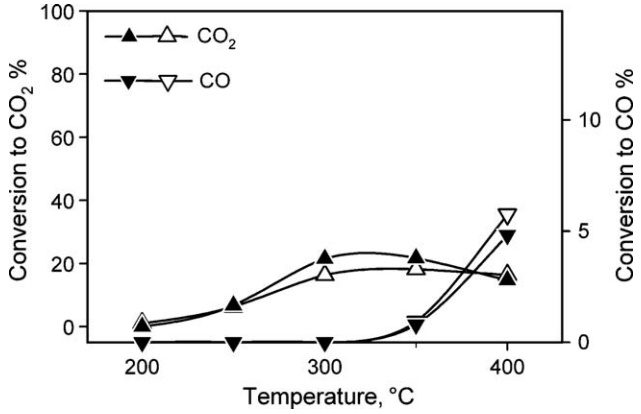

Fig. 9. CH_3OH conversion to CO_2 and CO in the SRM tests. Empty symbols (▽, △): catalyst pre-reduced with H_2; full symbols (▼, ▲): catalyst not pre-reduced.

attributed to the alumina phase, that is present in high amount and to the high surface area of the sample, since it is known that acid sites of alumina greatly activate the dehydration of methanol [33]. This reaction occurs in lower extent under OSRM conditions due to the competition with steam reforming. It can be supposed that also in this case metallic Cu is present even in the not pre-reduced sample, due to the reducing action of the reaction medium, but the activity of metallic Cu is so low under these conditions that no influence of the previous H_2 treatment can be detected. On the other hand, the activity of our catalyst under SRM conditions is not very different from that observed with other Cu/Ce/(Al) catalysts cited in the literature, although a precise comparison is hindered by differences in space velocities and catalyst compositions. From data in Table 4, the activity for simple SRM of our catalyst appears comparable to that of Cu/Ce/(Al) catalysts previously reported, if differences in Cu loading and partial pressures of the reactants are taken into account.

The present results, in agreement with literature data, indicate that when oxygen is absent from the feed, the activity of the

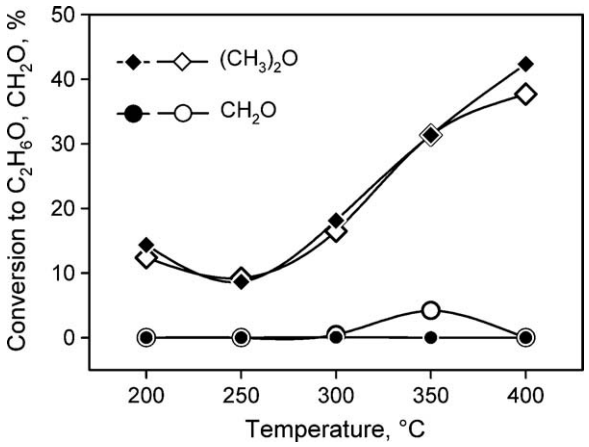

Fig. 10. CH_3OH conversion to $(CH_3)_2O$ and CH_2O in the SRM tests. Empty symbols (◇, ○): catalyst pre-reduced with H_2; full symbols (◆, ●): catalyst not pre-reduced.

$EMCe_{14}Cu_7$ catalyst for SRM is lower than that of more traditional $Cu/ZnO/(Al_2O_3)$ systems. This difference can be due to the effect of the ZnO phase. It is known that ZnO is an effective promoter of Cu based catalysts for synthesis or reforming of CH_3OH: different interpretations of such effect are given, such as stabilization of Cu(I) in a mixed Cu/Zn oxide [65], formation of a surface Cu/Zn alloy [66], increase of disorder and microstrain in Cu particles [67], H spillover effects [68]. It clearly appears that CeO_2 is not able to give a similar promoter effect under SRM conditions. On the other hand, when O_2 is present in the feed, the activity of $EMCe_{14}Cu_7$ for methanol reforming is highly enhanced and becomes similar to that of traditional $Cu/ZnO/(Al_2O_3)$ systems. A possible explanation of this behaviour is that ceria promotes the reaction through a mechanism of H spillover. The rate determining step of methanol reforming is probably the abstraction of H atoms from adsorbed methanol or some other adsorbed species [8], so the reaction rate can be increased if a hydrogen spillover effect occurs on the oxide matrix. Such effect was observed with other CeO_2 supported catalysts, such as Pt/CeO_2 or Cu/CeO_2 [69,70] and can most probably occur on the present system due to the very high dispersion of metallic Cu. The adsorption of H atoms on CeO_2 can lead to the reaction:

$$Ce^{4+}-O-Ce^{4+} + H \leftrightarrows Ce^{3+}-O(H)-Ce^{4+} \quad (5)$$

The last species can be considered a storage form of H, from which H can be obtained by the reverse reaction. When the catalyst is exposed to a reducing system such as the SRM feed, reaction (5) can lead to complete reduction of Ce^{4+} to Ce^{3+}, in this way the spillover effect is impaired and the rate of reforming decreases. On the other hand, when some O_2 is present in the feed, cerium can be maintained, at least partially, in the oxidized Ce^{4+} state and spillover can occur.

A different explanation is based on the possible oxidation of Cu in the presence of CeO_2, according to the reaction (6) [64]:

$$Ce^{4+} + Cu \rightarrow Ce^{3+} + Cu^{+} \quad (6)$$

Table 4
Comparison of data from SRM tests.

Author [reference]	Catalyst composition Cu/Ce/Al (atom %)	Feed ratio H_2O/CH_3OH	WHSV (L g^{-1} h^{-1})	Temperature (°C)	H_2 production rate (μmol s^{-1} g_{cat}^{-1})
Present work	6/6/88	1.1/1	60	250	20
Liu et al. [64]	10/90/0	1/1	5	240	40
Zhang and Shi [50]	25/8/67	1/1	8	250	83

The above TPR data suggest that CeO_2 favours the Cu^+ oxidation state, in agreement with previous works [35,59]. Moreover XPS measurements effected on the used catalysts gives evidence of the presence of Cu^+ species [Turco et al., unpublished data]. The presence of Cu^+ under steam reforming conditions was also reported for other Cu based catalysts and found essential for the reaction [71,72]. It is possible that Cu^+, together with Cu^0, has an active role in the steam reforming of methanol [8,23,73], probably through the formation of Cu^+–O–Cu^+ sites on the surface of metallic Cu. Such sites are involved in methanol chemisorption, that is a key step in the mechanism of methanol reforming [8]. It can be supposed that oxygen re-oxidizes Ce^{3+} to Ce^{4+}, thus allowing reaction (6) to proceed, this leads to a faster restoring of Cu^+ sites and can explain a much higher activity for SRM in the presence of O_2.

4. Conclusions

The present data have confirmed that the new single-step sol–gel method is effective to prepare high surface area mesostructured Cu/Ce/Al oxide systems. Copper oxide is present in a highly dispersed form in this material, and gives, after reduction, a nanometric metallic phase with an exceptionally high surface area.

Catalytic tests have shown a noticeable activity for the OSRM process also of the material not pre-reduced with H_2, indicating that the metallic phase, although with lower activity, can be formed directly under reaction conditions. The different catalytic performances observed in OSRM and SRM tests have indicated a strong influence of the presence of O_2 in the reaction system. This has been explained hypothesizing that CeO_2 plays an important role in the methanol reforming catalytic process, but O_2 is needed to maintain the Ce^{4+} oxidation state.

Acknowledgement

The authors acknowledge the financial support of MIUR (Ministero Italiano Università Ricerca).

References

[1] C. Song, Catal. Today 77 (2002) 17.
[2] D.D. Boettner, M.J. Moran, Energy 29 (2004) 2317.
[3] D.R. Palo, R.A. Dagle, J.D. Holladay, Chem. Rev. 107 (2007) 3992.
[4] R.M. Navarro, M.A. Peña, J.L.G. Fierro, Chem. Rev. 107 (2007) 3952.
[5] J.R. Lattner, M.P. Harold, Catal. Today 120 (2007) 78.
[6] D. Trimm, Z. Onsan, Cat. Rev. Sci. Eng. 43 (2001) 39.
[7] J.R. Lattner, M.P. Harold, Appl. Catal. B: Environ. 56 (2005) 149.
[8] M. Turco, G. Bagnasco, C. Cammarano, P. Senese, U. Costantino, M. Sisani, Appl. Catal. B: Environ. 77 (2007) 46.
[9] M. Turco, G. Bagnasco, U. Costantino, F. Marmottini, T. Montanari, G. Ramis, G. Busca, J. Catal. 228 (2004) 56.
[10] D.L. Trimm, Appl. Catal. A: Gen. 296 (2005) 1.
[11] R.J. Farrauto, Appl. Catal. B: Environ. 56 (2005) 3.
[12] S. Liu, K. Takahashi, K. Uematsu, M. Ayabe, Appl. Catal. A: Gen. 283 (2005) 125.
[13] N. Iwasa, W. Nomura, T. Mayanagi, S. Fujita, M. Arai, N. Takezawa, J. Chem. Eng. Jpn. 37 (2004) 286.
[14] M.L. Cubeiro, J.L.G. Fierro, J. Catal. 179 (1998) 150.
[15] M. Lenarda, L. Storaro, R. Frattini, M. Casagrande, M. Marchiori, G. Capannelli, C. Uliana, F. Ferrari, R. Ganzerla, Catal. Commun. 8 (2007) 467.
[16] M. Lenarda, E. Moretti, L. Storaro, P. Patrono, F. Pinzari, E. Rodríguez-Castellón, A. Jiménez-López, G. Busca, E. Finocchio, T. Montanari, R. Frattini, Appl. Catal. A: Gen. 312 (2006) 220.
[17] A. Karim, T. Conant, A. Datye, J. Catal. 243 (2006) 420.
[18] S. Liu, K. Takahashi, K. Fuchigami, K. Uematsu, Appl. Catal. A: Gen. 299 (2006) 58.
[19] S. Fukahori, T. Kitaoka, A. Tomoda, R. Suzuki, H. Wariishi, Appl. Catal. A: Gen. 300 (2006) 155.
[20] F. Raimondi, B. Schnyder, R. Kotz, R. Schelldorfer, T. Jung, J. Wambach, A. Wokaun, Surf. Sci. 532–535 (2003) 383.
[21] T.L. Reitz, P.L. Lee, K.F. Czaplewski, J.C. Lang, K.E. Popp, H.H. Kung, J. Catal. 199 (2001) 193.
[22] K. Geissler, E. Newson, F. Vogel, T.B. Truong, P. Hottinger, A. Wokaun, Phys. Chem. Chem. Phys. 3 (2001) 289.
[23] S. Murcia-Mascarós, R.M. Navarro, L. Gómez-Sainero, U. Costantino, M. Rocchetti, J.L.G. Fierro, J. Catal. 198 (2001) 338.
[24] S. Velu, K. Suzuki, M. Okazaki, M.P. Kapoor, T. Osaki, F. Ohashi, J. Catal. 194 (2000) 373.
[25] T.L. Reitz, S. Ahmed, M. Krumpelt, R. Kumar, H.H. Kung, J. Mol. Catal. A: Chem. 162 (2000) 275.
[26] U. Costantino, F. Marmottini, M. Sisani, T. Montanari, G. Ramis, G. Busca, M. Turco, M. Bagnasco, Solid State Ionics 176 (2005) 39.
[27] M. Turco, G. Bagnasco, U. Costantino, F. Marmottini, T. Montanari, G. Ramis, G. Busca, J. Catal. 228 (2004) 43.
[28] C. Horny, L. Kiwi-Minsker, A. Renken, Chem. Eng. J. 101 (2004) 3.
[29] J.K. Lee, J.B. Ko, D.H. Kim, Appl. Catal. A: Gen. 278 (2004) 25.
[30] S. Catillon, C. Louis, R. Rouget, Top. Catal. 30/31 (2004) 463.
[31] R. Pérez-Hernandez, A. Gutiérrez-Martinez, C.E. Gutiérrez–Wing, Int. J. Hydrogen Energy 32 (2007) 2888.
[32] S. Patel, K.K. Pant, J. Power Sources 159 (2006) 139.
[33] Y. Men, H. Gnaser, R. Zapf, V. Hessel, C. Ziegler, G. Kolb, Appl. Catal. A: Gen. 277 (2004) 83.
[34] Y. Liu, T. Hayakawa, T. Tsunoda, K. Suzuki, S. Hamakawa, K. Murata, R. Shiozaki, T. Ishii, M. Kumagai, Top. Catal. 22 (2003) 205.
[35] Y. Liu, T. Hayakawa, K. Suzuki, S. Hamakawa, T. Tsunoda, T. Ishii, M. Kumagai, Appl. Catal. A: Gen. 223 (2002) 137.
[36] C.-Y. Shiau, M.W. Ma, C.S. Chuang, Appl. Catal. A: Gen. 301 (2006) 89.
[37] G. Marbán, A.B. Fuertes, Appl. Catal. B: Environ. 57 (2005) 43.
[38] S. Patel, K.K. Pant, Fuel Process. Technol. 88 (2007) 825.
[39] L. Li, Y. Zhan, Q. Zheng, Y. Zheng, X. Lin, J. Zhu, Catal. Lett. 118 (2007) 91.
[40] Y. Li, Q. Fu, M. Flytzani-Stephanopoulos, Appl. Catal. B: Environ. 27 (2000) 179.
[41] B. Skårman, D. Grandjean, R.E. Benfield, A. Hinz, A. Andersson, L.R. Wallemberg, J. Catal. 211 (2002) 119.
[42] W. Shen, X. Dong, Y. Zhu, H. Chen, J. Shi, Microporous Mesoporous Mater. 85 (2005) 157.
[43] M.-F. Luo, J.-M. Ma, J.-Q. Lu, Y.-P. Song, Y.-J. Wang, J. Catal. 246 (2007) 52.
[44] S. Hočevar, U.O. Krašovec, B. Orel, A.S. Aricó, H. Kimd, Appl. Catal. B: Environ. 28 (2000) 113.
[45] Y. Liu, Q. Fu, M.F. Stephanopoulos, Catal. Today 93–95 (2004) 241.
[46] A. Martínez-Arias, M. Fernández-García, O. Gálvez, J.M. Coronado, J.A. Anderson, J.C. Conesa, J. Soria, G. Munuera, J. Catal. 195 (2000) 207.
[47] D.H. Kim, J.E. Cha, Catal. Lett. 86 (2003) 107.
[48] Z. Liu, R. Zhou, X. Zheng, J. Mol. Catal A: Chem. 267 (2007) 137.
[49] E. Moretti, M. Lenarda, L. Storaro, A. Talon, T. Montanari, G. Busca, E. Rodríguez-Castellón, A. Jiménez-López, M. Turco, G. Bagnasco, R. Frattini, Appl. Catal. A: Gen. 335 (2008) 46.
[50] X. Zhang, P. Shi, J. Mol. Catal. A: Chem. 194 (2003) 99.
[51] G. Avgouropoulos, T. Ioannides, H. Matralis, Appl. Catal. B: Environ. 56 (2005) 87.
[52] A. Pintar, J. Batista, S. Hočevar, J. Colloid Interface Sci. 285 (2005) 218.
[53] E. Moretti, M. Lenarda, L. Storaro, R. Frattini, P. Patrono, F. Pinzari, J. Colloid Interface Sci. 306 (2007) 89.
[54] G.C. Bond, S.N. Namijo, J. Catal. 118 (1989) 507.
[55] F. Giordano, A. Trovarelli, C. de Leitemburg, M. Giona, J. Catal. 193 (2000) 273.
[56] E. Aneggi, M. Boaro, C. de Leitemburg, G. Dolcetti, A. Trovarelli, J. Alloys Compd. 408 (2006) 1096.
[57] M.C. Cabús-Llaurado, Y. Cesteros, F. Medina, P. Salagre, J.E. Sueiras, Microporous Mesoporous Mater. 100 (2007) 167.
[58] X. Courtois, V. Perrichon, M. Primet, G. Bergeret, in: A. Corma, F.V. Melo, S. Mendioroz, J.L.G. Fierro (Eds.), Stud. Surf. Sci. Catal. 130B (2000) 1031.
[59] A. Martinez-Arias, J.C. Cataluña, J.C. Conesa, J. Soria, J. Phys. Chem. B 102 (1998) 809.
[60] S. Patel, K.K. Pant, Appl. Catal. A: Gen. 356 (2009) 189.
[61] W. Shan, Z. Feng, Z. Li, J. Zhang, W. Shen, C. Li, J. Catal. 228 (2004) 206.
[62] P.B. Malla, P. Ravindranathan, S. Komarneni, E. Breval, R. Roy, J. Mater. Chem. 2 (1992) 559.
[63] F. Kooli, V. Rives, W. Jones, Chem. Mater. 9 (1997) 2231.
[64] Y. Liu, T. Hayakawa, K. Suzuki, S. Hamakawa, Catal. Commun. 2 (2001) 195.
[65] A.A. Khassin, V.V. Pelipenko, T.P. Minyukova, V.I. Zaikovskii, D.I. Kochubey, T.M. Yurieva, Catal. Today 112 (2006) 143.
[66] E.D. Batyrev, J.C. van den Heuvel, J. Beckers, W.P.A. Jansen, H.L. Castricum, J. Catal. 229 (2005) 136.
[67] M.M. Günter, T. Ressler, R.E. Jentoft, B. Bems, J. Catal. 203 (2001) 133.
[68] R. Burch, S.E. Golunski, M.S. Spencer, Catal. Lett. 5 (1990) 55.
[69] W. Lin, A.A. Herzing, C.J. Kiely, I.E. Wachs, J. Phys. Chem. C 112 (2008) 5942.
[70] K.A. Pokrovski, A.T. Bell, J. Catal. 241 (2006) 276.
[71] G.-S. Wu, D.-S. Mao, G.Z. Lu, Y. Cao, K.N. Fan, Catal. Lett. 130 (2009) 177.
[72] S.D. Jones, L.M. Neal, H.E. Hagelin-Weaver, Appl. Catal. B: Environ. 84 (2008) 631.
[73] F. Raimondi, K. Geissler, J. Wambach, A. Wokaun, Appl. Surf. Sci. 189 (2002) 59.